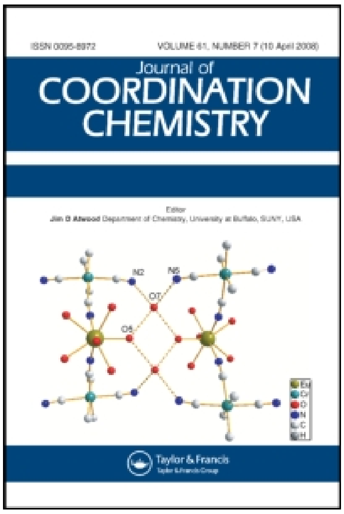

Journal of Coordination Chemistry

Publication details, including instructions for authors and subscription information:
http://www.informaworld.com/smpp/title~content=t713455674

Synthesis, crystal structure and properties of two terbium complexes with 2,2'-bipyridine

Xia Li[a]; Yan-Ling Ju[a]; Yan-Qiu Li[a]
[a] Department of Chemistry, Capital Normal University, Beijing, P. R. China

To cite this Article Li, Xia , Ju, Yan-Ling and Li, Yan-Qiu(2008) 'Synthesis, crystal structure and properties of two terbium complexes with 2,2'-bipyridine', Journal of Coordination Chemistry, 61: 5, 692 — 704, First published on: 20 July 2007 (iFirst)

To link to this Article: DOI: 10.1080/00958970701390011

URL: http://dx.doi.org/10.1080/00958970701390011

Journal of Coordination Chemistry
Vol. 61, No. 5, 10 March 2008, 692–704

Synthesis, crystal structure and properties of two terbium complexes with 2,2′-bipyridine

XIA LI*, YAN-LING JU and YAN-QIU LI

Department of Chemistry, Capital Normal University,
Beijing 100037, P. R. China

(*Received 8 March 2007; in final form 12 May 2007*)

Two new complexes {[Tb(2-IBA)$_3\cdot$2,2′-bipy]$_2\cdot C_2H_5OH$} (**1**) and [Tb(2-ClBA)$_3\cdot$2,2′-bipy]$_2$ (**2**) (2-IBA = 2-iodobenzoate; 2-ClBA = 2-chlorobenzoate; 2,2′-bipy = 2,2′-bipyridine) were prepared and their crystal structures determined by X-ray diffraction. Complex **1** is composed of two types of binuclear molecules, [Tb(2-IBA)$_3\cdot$2,2′-bipy]$_2$ (a) and [Tb(2-IBA)$_3\cdot$2,2′-bipy]$_2$ (b), and an uncoordinated ethanol molecule. In molecule (a), two Tb^{3+} ions are linked by four 2-IBA groups, all bidentate-bridging. In molecule (b), two Tb^{3+} ions are held together by four 2-IBA groups in two coordination modes, bidentate-bridging and chelating-bridging. In the two molecules, each Tb^{3+} ion is further bonded to one chelating 2-IBA group and one chelating 2,2′-bipy molecule, resulting in coordination numbers of eight for (a) and nine for (b). The structural characteristics of **2** are similar to that of molecule (b) in **1**. The two complexes, **1** and **2**, both emit strong green fluorescence under ultraviolet light with the $^5D_4 \rightarrow {}^7F_j$ ($j = 6$–3) emission of Tb^{3+} ion observed.

Keywords: Terbium complexes; 2-Iodobenzoic acid; 2-Chlorobenzoic acid; Crystal structure

1. Introduction

In the 1840s, Weissman [1] found that near ultraviolet light excites some lanthanide complexes with organic ligands containing conjugated systems, which then emit fluorescence. Fluorescent lanthanide complexes have been a very active area; most terbium complexes emit green fluorescence and have many applications [2–14]. Terbium mono-aromatic acid complexes have been studied because these complexes have various structures and intense characteristic fluorescence [5–14]. For example, terbium benzoic acid (HBA) complexes containing 2,2′-bipyridine (2,2′-bipy) and 1,10-phenanthroline (phen), [Tb(BA)$_3$(2,2′-bipy)]$_2$ [11] and [Tb(BA)$_3$(phen)]$_2$ [12], have been studied. Furthermore, terbium complexes of benzoic acid derivatives have been reported, [Tb(2-FBA)$_3\cdot$2,2′-bipy]$_2$ (2-FBA = 2-fluorobenzoate) [13] and [Tb(2-MBA)$_3$(phen)]$_2$

---

*Corresponding author. Email: xiali@mail.cnu.edu.cn

Journal of Coordination Chemistry
ISSN 0095-8972 print/ISSN 1029-0389 online © 2008 Taylor & Francis
DOI: 10.1080/00958970701390011

(2-MBA = 2-methylbenzoate) [14]. Lanthanide carboxylate complexes have many structures owing to monodentate, bidentate chelating, bidentate bridging, and chelating–bridging coordination modes of carboxylates. Different carboxylate ligands containing a second ligand (2,2′-bipy or phen) may arouse different structural characters. We are interested in the structure of complexes with different substituents in the benzene ring of benzoic acid. Two new terbium complexes with 2-iodobenzoic acid (2-HIBA) and 2-chlorobenzoic acid (2-HClBA) containing 2,2′-bipy, $\{[Tb(2\text{-}IBA)_3 \cdot 2,2'\text{-bipy}]_2 \cdot C_2H_5OH\}$ (**1**) and $[Tb(2\text{-}ClBA)_3 \cdot 2,2'\text{-bipy}]_2$ (**2**), were synthesized and their crystal structures and luminescence properties investigated.

2. Experimental

2.1. *Materials and methods*

$TbCl_3 \cdot 6H_2O$ was prepared by dissolving its oxides in hydrochloric acid and then drying the solution. Elemental analysis was performed on an Elementar Vario EL analyzer. IR spectra were recorded with a Bruker EQUINOX-55 using the KBr pellets. Fluorescence spectra were measured on a F-4500 FL spectrophotometer in the solid state at room temperature. UV spectra were measured on a TU-1810 spectrophotometer. Thermogravimetric analysis was performed on a WCT-1A thermal analyzer at a heating rate of $10^{\circ}C\,min^{-1}$ in air.

2.2. *Synthesis of the complexes*

1.2 mmol 2-iodobenzoic acid or 2-chlorobenzoic acid, 0.4 mmol 2,2′-bipyridine and 0.4 mmol $TbCl_3 \cdot 6H_2O$ were dissolved in 25 mL ethanol. The pH of the solution was adjusted to 6 ~ 7 with $2\,mol\,L^{-1}$ NaOH solution. The mixture was heated under reflux with stirring for 2 h and the resulting solution was filtered and left to stand at room temperature for two weeks. Colourless single crystals were obtained from the mother liquor. Yield, about 52%. For **1**, $C_{64}H_{46}I_6Tb_2N_4O_{12}$ (2158.31), Calcd (%): C, 35.62; H, 2.15; N, 2.59. Found (%): C, 35.55; H, 2.20; N, 2.45. Selected IR (KBr pellet, ν/cm^{-1}): 1617 *vs*, 1590 s, 1545 m, 1475 m, 1405 vs, 1051 m, 858 m, 751 s, 729 m, 649 m, 461 m, 417 w. For **2**, $C_{62}H_{40}Cl_6Tb_2N_4O_{12}$ (1563.52), Calcd (%): C, 47.63; H, 2.58; N, 3.58. Found (%): C, 47.58; H, 2.58; N, 3.46. Selected IR (KBr pellet, ν/cm^{-1}): 1614 *vs*, 1580 s, 1547 m, 1477 m, 1435 s, 1406 vs, 1052 m, 1013 m, 858 m, 752 s, 649 m, 460 m, 411 w.

2.3. *X-ray crystallographic study*

X-ray crystal data collection for the complexes is on a Bruker Smart 1000CCD diffractometer with monochromated Mo-Kα radiation ($\lambda = 0.71073$ Å) at 293 K. Semi-empirical absorption corrections were applied using the SADABS program. All calculations were carried out on a computer with use of SHELXS-97 and SHELXL-97 programs [15, 16]. The structures were solved by direct methods and refinement on $|F|^2$ used the full-matrix least-squares methods. Summary of the crystallographic data and details of the structure refinements are listed in table 1. Selected bond lengths and angles of **1** and **2** are listed in tables 2 and 3, respectively.

Table 1. Crystal data and experimental details of the complexes.

Complex	**1**	**2**
Chemical formula	$C_{64}H_{46}I_6N_4O_{13}Tb_2$	$C_{62}H_{40}Cl_6N_4O_{12}Tb_2$
Formula weight	2158.31	1563.54
Temperature (K)	293(2)	293(2)
Wavelength (Å)	0.71073	0.71073
Crystal system	Triclinic	Triclinic
Space group	$P\bar{1}$	$P\bar{1}$
a (Å)	11.6415(2)	11.3322(6)
b (Å)	13.9861(3)	12.3125(7)
c (Å)	21.2074(4)	12.8349(7)
α (°)	86.1030(10)	63.915(3)
β (°)	87.6240(10)	68.774(3)
γ (°)	76.2710(10)	80.844(3)
Volume ($Å^3$)	3345.42(11)	1499.30(15)
Z	2	1
Calculated density ($mg\,m^{-3}$)	2.143	1.732
Absorption coefficient (mm^{-1})	4.929	2.673
$F(000)$	2020.0	768.0
Crystal size (mm^3)	$0.40 \times 0.25 \times 0.15$	$0.40 \times 0.25 \times 0.15$
θ range (°)	0.96 to 28.41	1.84 to 28.35
Limiting indices	$-15 \le h \le 15$, $-18 \le k \le 18$, $-28 \le l \le 28$	$-12 \le h \le 15$, $-13 \le k \le 16$, $-14 \le l \le 17$
Reflections collected/unique	47238/16810 [$R_{(int)} = 0.0497$]	19312/15002 [$R_{(int)} = 0.0194$]
Data/restraints/parameters	16386/0/804	10009/3/763
Goodness-of-fit on F^2	0.982	1.131
Final R indices [$I > 2\sigma(I)$]	$R_1 = 0.0552$, $wR_2 = 0.1534$	$R_1 = 0.0263$, $wR_2 = 0.0704$
R indices (all data)	$R_1 = 0.1021$, $wR_2 = 0.1688$	$R_1 = 0.0310$, $wR_2 = 0.0727$
Largest diff. peak and hole ($e\,Å^{-3}$)	4.065 and −3.255	1.842 and −1.043

Table 2. Selected bond lengths (Å) and angles (°) of **1**.

Tb(1)–O(6)#1	2.325(5)	Tb(1)–O(1)#1	2.345(5)
Tb(1)–O(2)	2.358(5)	Tb(1)–O(4)	2.386(5)
Tb(1)–O(3)	2.424(6)	Tb(1)–O(5)	2.450(6)
Tb(1)–N(3)	2.541(7)	Tb(1)–N(2)	2.602(7)
Tb(2)–O(12)#2	2.330(6)	Tb(2)–O(7)#2	2.339(6)
Tb(2)–O(11)	2.359(6)	Tb(2)–O(10)	2.395(6)
Tb(2)–O(9)	2.412(7)	Tb(2)–O(8)	2.446(7)
Tb(2)–O(7)	2.659(6)	Tb(2)–N(1)	2.605(8)
Tb(2)–N(4)	2.556(9)		
O(6)#1–Tb(1)–O(1)#1	74.0(2)	O(6)#1–Tb(1)–O(2)	78.4(2)
O(1)#1–Tb(1)–O(2)	130.30(19)	O(6)#1–Tb(1)–O(4)	125.0(2)
O(1)#1–Tb(1)–O(4)	85.7(2)	O(2)–Tb(1)–O(4)	77.4(2)
O(6)#1–Tb(1)–O(3)	91.9(2)	O(1)#1–Tb(1)–O(3)	92.3(2)
O(2)–Tb(1)–O(3)	129.42(19)	O(4)–Tb(1)–O(3)	140.4(2)
O(6)#1–Tb(1)–O(5)	78.8(2)	O(1)#1–Tb(1)–O(5)	135.2(2)
O(2)–Tb(1)–O(5)	75.9(2)	O(4)–Tb(1)–O(5)	139.0(2)
O(3)–Tb(1)–O(5)	53.6(2)	N(3)–Tb(1)–N(2)	62.9(2)
O(12)#2–Tb(2)–O(7)#2	74.3(2)	O(12)#2–Tb(2)–O(11)	134.7(2)
O(7)#2–Tb(2)–O(11)	75.7(2)	O(12)#2–Tb(2)–O(10)	127.8(2)
O(7)#2–Tb(2)–O(10)	81.2(2)	O(11)–Tb(2)–O(10)	79.0(2)
O(12)#2–Tb(2)–O(9)	83.5(3)	O(7)#2–Tb(2)–O(9)	124.8(2)
O(11)–Tb(2)–O(9)	86.6(3)	O(10)–Tb(2)–O(9)	146.1(3)
O(12)#2–Tb(2)–O(8)	78.2(2)	O(7)#2–Tb(2)–O(8)	81.2(2)
O(11)–Tb(2)–O(8)	129.0(2)	O(10)–Tb(2)–O(8)	52.6(2)
O(9)–Tb(2)–O(8)	142.4(3)	O(12)#2–Tb(2)–O(7)	69.6(2)
O(7)#2–Tb(2)–O(7)	74.0(2)	O(11)–Tb(2)–O(7)	70.0(2)
O(10)–Tb(2)–O(7)	144.1(2)	O(9)–Tb(2)–O(7)	50.9(2)
O(8)–Tb(2)–O(7)	143.5(2)	N(4)–Tb(2)–N(1)	61.1(3)

Symmetry transformations used to generate equivalent atoms: #1: $-x+2$, $-y$, $-z+1$; #2: $-x+1$, $-y+1$, $-z$.

Table 3. Selected bond lengths (Å) and angles (°) of **2**.

Tb(1)–O(3)	2.328(10)	Tb(1)–O(9)	2.348(9)
Tb(1)–O(1)	2.373(10)	Tb(1)–O(7)	2.433(11)
Tb(1)–O(8)	2.428(12)	Tb(1)–O(11)	2.475(10)
Tb(1)–O(12)	2.586(10)	Tb(1)–N(1)	2.536(12)
Tb(1)–N(2)	2.612(11)	Tb(2)–O(12)	2.343(10)
Tb(2)–O(2)	2.352(9)	Tb(2)–O(4)	2.362(10)
Tb(2)–O(10)	2.461(11)	Tb(2)–O(6)	2.427(12)
Tb(2)–O(5)	2.427(10)	Tb(2)–O(9)	2.660(11)
Tb(2)–N(3)	2.646(12)	Tb(2)–N(4)	2.535(10)
O(3)–Tb(1)–O(9)	74.9(4)	O(3)–Tb(1)–O(1)	134.7(4)
O(9)–Tb(1)–O(1)	76.1(4)	O(3)–Tb(1)–O(7)	130.1(4)
O(9)–Tb(1)–O(7)	79.4(3)	O(1)–Tb(1)–O(7)	76.3(4)
O(3)–Tb(1)–O(8)	80.4(4)	O(9)–Tb(1)–O(8)	81.3(4)
O(1)–Tb(1)–O(8)	128.1(4)	O(7)–Tb(1)–O(8)	53.7(4)
O(3)–Tb(1)–O(11)	86.2(4)	O(9)–Tb(1)–O(11)	124.8(3)
O(1)–Tb(1)–O(11)	82.6(4)	O(7)–Tb(1)–O(11)	142.7(3)
O(8)–Tb(1)–O(11)	146.2(4)	O(3)–Tb(1)–O(12)	67.8(4)
O(9)–Tb(1)–O(12)	73.9(3)	O(1)–Tb(1)–O(12)	71.1(3)
O(7)–Tb(1)–O(12)	141.8(3)	O(8)–Tb(1)–O(12)	143.6(4)
O(11)–Tb(1)–O(12)	51.0(3)	O(12)–Tb(2)–O(2)	75.6(3)
N(2)–Tb(1)–N(1)	62.0(4)	O(12)–Tb(2)–O(4)	75.1(3)
O(2)–Tb(2)–O(4)	135.4(3)	O(12)–Tb(2)–O(6)	82.2(4)
O(2)–Tb(2)–O(6)	127.5(3)	O(4)–Tb(2)–O(6)	80.3(4)
O(12)–Tb(2)–O(5)	82.9(3)	O(2)–Tb(2)–O(5)	76.6(4)
O(4)–Tb(2)–O(5)	131.2(4)	O(6)–Tb(2)–O(5)	53.6(3)
O(12)–Tb(2)–O(10)	123.1(4)	O(2)–Tb(2)–O(10)	83.2(4)
O(4)–Tb(2)–O(10)	85.5(4)	O(6)–Tb(2)–O(10)	146.5(4)
O(5)–Tb(2)–O(10)	141.7(3)	O(12)–Tb(2)–O(9)	72.6(3)
O(2)–Tb(2)–O(9)	71.7(3)	O(4)–Tb(2)–O(9)	67.9(4)
O(6)–Tb(2)–O(9)	143.3(3)	O(5)–Tb(2)–O(9)	143.7(3)
O(10)–Tb(2)–O(9)	50.7(3)	O(12)–Tb(2)–O(9)	72.6(3)
O(2)–Tb(2)–O(9)	71.7(3)	O(4)–Tb(2)–O(9)	67.9(4)
O(6)–Tb(2)–O(9)	143.3(3)	O(5)–Tb(2)–O(9)	143.7(3)
O(10)–Tb(2)–O(9)	50.7(3)	N(4)–Tb(2)–N(3)	63.4(3)

Symmetry transformations used to generate equivalent atoms: *x*, *y*, *z*.

3. Results and discussion

3.1. *Structural description of complexes*

The complex $\{[\mathrm{Tb(2\text{-}IBA)}_3\cdot 2,2'\text{-bipy}]_2\cdot \mathrm{C_2H_5OH}\}$ (**1**) consists of two independent molecules $[\mathrm{Tb(2\text{-}IBA)}_3\cdot 2,2'\text{-bipy}]_2$ (a) (figure 1a) and $[\mathrm{Tb(2\text{-}IBA)}_3\cdot 2,2'\text{-bipy}]_2$ (b) (figure 1b), and one uncoordinated ethanol. Molecules (a) and (b) form a centrosymmetric dimeric unit. In (a), the two central metal ions (Tb1 and Tb1A) are linked by four bidentate bridging 2-IBA groups. Each central Tb1^{3+} ion is also chelated by one 2-IBA group and one 2,2′-bipy, forming a coordination number of eight. The Tb1^{3+} ion is in a distorted square-antiprism coordination environment with six oxygen atoms from five 2-IBA ligands and two nitrogen atoms from one 2,2′-bipy (figure 2a). The upper and lower squares are made up of atoms O1A, O2, O4, O6A, and O3, O5, N2 and N3 with mean deviations of 0.0524 and 0.2244 Å, respectively. The dihedral angle between the two squares is 7.4°. In (b), the two central metal ions (Tb2 and Tb2A) are connected through four 2-IBA groups by bidentate bridging and chelating–bridging coordination modes. Each Tb2^{3+} ion is further bonded to two oxygen atoms of one chelated 2-IBA group and two nitrogens of one 2,2′-bipy, forming a coordination

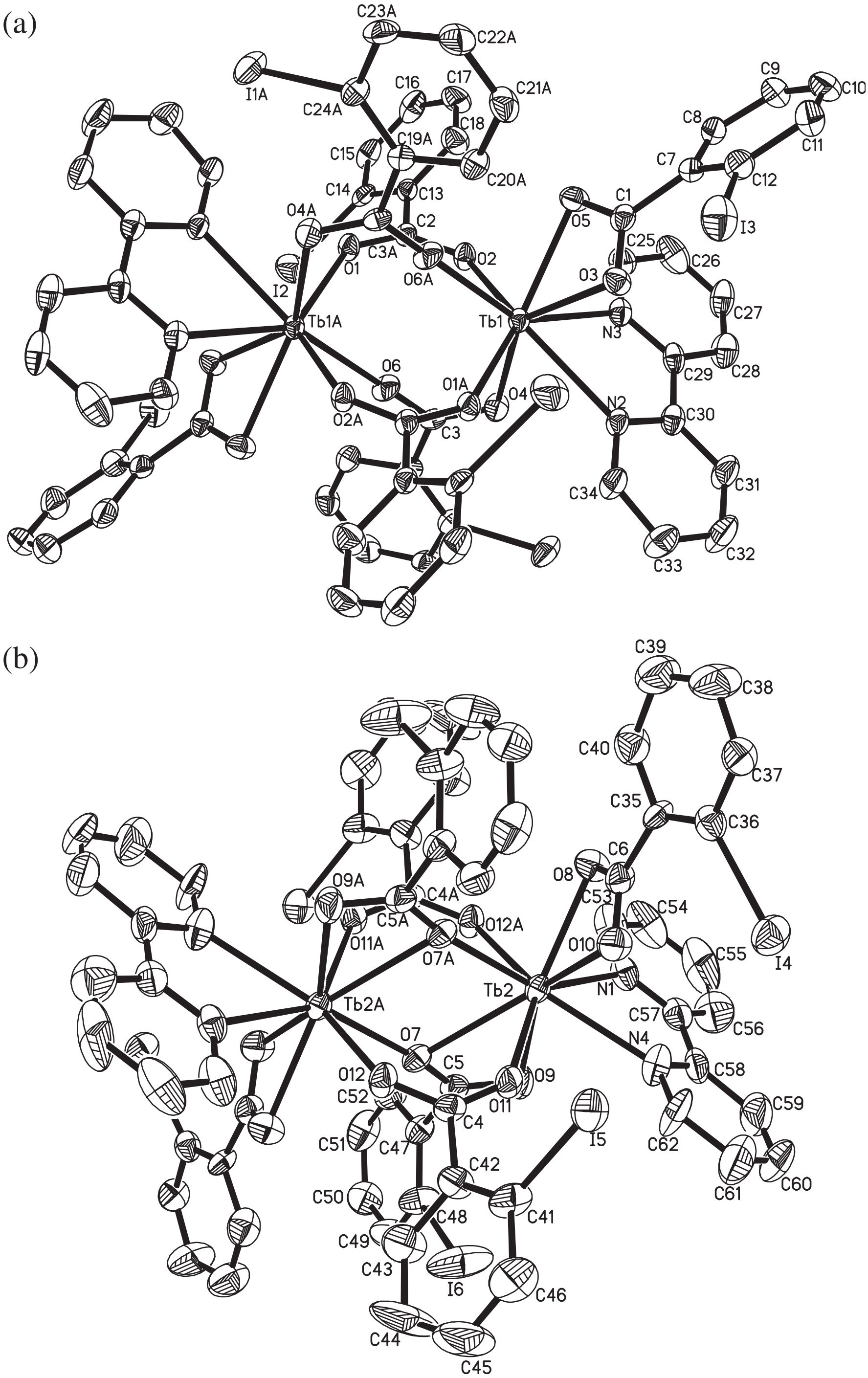

Figure 1. (a) and (b) show two structures of **1** in the asymmetric unit. One uncoordinated ethanol molecule and all hydrogen atoms are omitted for clarity; the thermal ellipsoids are shown at the 30% probability level.

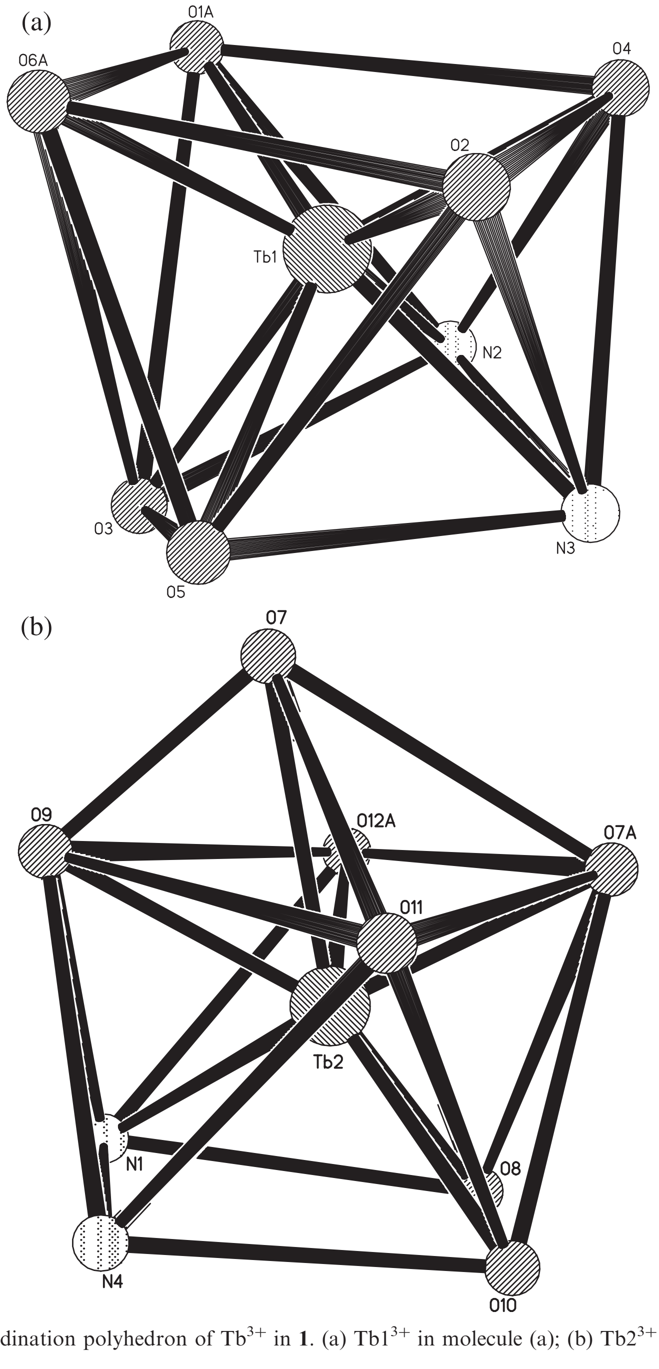

Figure 2. Coordination polyhedron of Tb^{3+} in **1**. (a) $Tb1^{3+}$ in molecule (a); (b) $Tb2^{3+}$ in molecule (b).

number of nine. The coordination environment of $Tb2^{3+}$ is a distorted monocapped square-antiprism (figure 2b) in which the top square face is defined by atoms O7A, O9, O11, O12A and the bottom one is formed by O8, O10, N1, N4 with mean deviations of 0.1111 and 0.242 Å, respectively. The dihedral angle between the two squares is 7.4°.

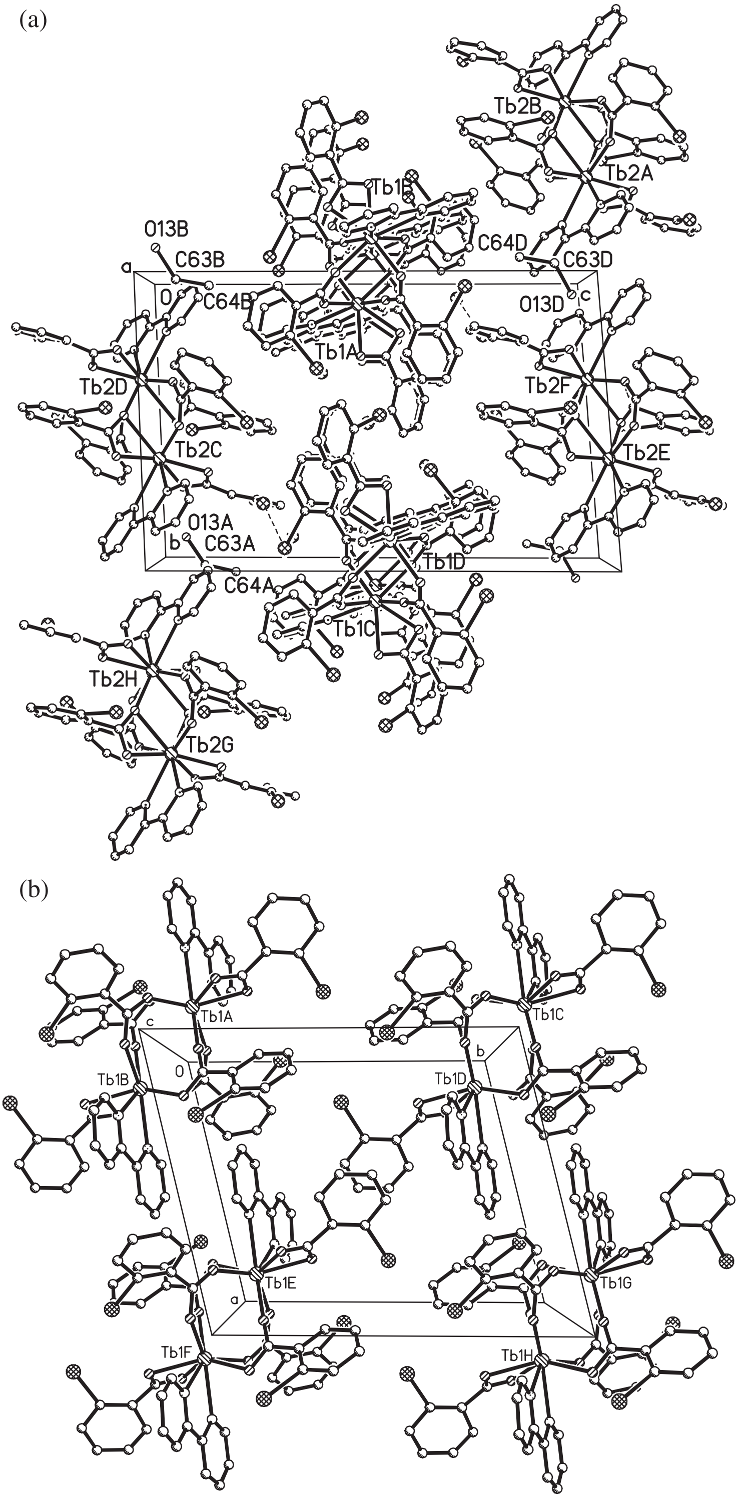

Figure 3. Packing diagram of **1**. (a) Viewed along *a*-axis; (b) Viewed along *c*-axis.

Atom O7 caps the upper plane. In (a) and (b), the 2,2′-bipy ligand chelates Tb^{3+} and are almost coplanar with dihedral angles of 3.3° and 6.3° (a) and (b), respectively.

In (a), Tb1–O bond distances range from 2.325(5)–2.450(6) Å with an average distance of 2.381 Å. The Tb1–N bond distances are 2.541(7) and 2.602(7) Å, respectively, with an average of 2.572 Å. The distance between two $Tb1^{3+}$ ions is 4.159(7) Å. In (b), Tb2–O bond distances range from 2.330(6)–2.659(6) Å with an average distance of 2.420 Å. The Tb2–N bond distances are 2.556(9) and 2.605(8) Å, respectively, with an average of 2.581 Å. The distance between two $Tb2^{3+}$ ions is 3.9972(8) Å. Obviously, d(Tb1–O) < d(Tb2–O) and d(Tb1–Tb1A) > d(Tb2–Tb2A) resulting from different bonding modes of carboxylate linking two Tb^{3+} ions in the two molecules. Ln^{3+} ions bridged by chelating-bridging carboxylate groups result in a larger Ln–O distance and a smaller Ln–Ln distance. The bond angles of O–Tb1–O for (a) and that of O–Tb2–O for (b) range from 53.6(2)–140.4(2)° and 52.6(2)–146.1(3)°, respectively. The bond angle of N2–Tb1–N3 for (a) and that of N1–Tb2–N4 for (b) are 62.9(2)° and 61.1(3)°, respectively.

Figure 3(a) shows the packing of **1** viewed along the *a*-axis, showing (a, Tb1) and (b, Tb2), and uncoordinated ethanol (C63C64O13) in the asymmetric unit. The distance of Tb^{3+} ions between (a) and (b) is 11.495(9) Å. Four atoms, Tb1, Tb1A, Tb2, and Tb2A, are almost coplanar with mean deviation from plane of 0.7981 Å. Viewed along the *b*-axis, the packing diagram of **1** displays the same structural features, but viewed along the *c*-axis only molecule (a, Tb1) is seen (figure 3b).

The structure of $[Tb(2\text{-ClBA})_3 \cdot 2,2'\text{-bipy}]_2$ (**2**) is shown in figure 4. Unlike **1**, **2** contains only one binuclear molecule in the asymmetric unit. The coordination environment of Tb^{3+} in **2** is similar to that of (b) in **1**. The nine-coordinated $Tb1^{3+}$ in **2** is bonded to seven oxygen atoms from the five 2-IBA groups and two nitrogen atoms

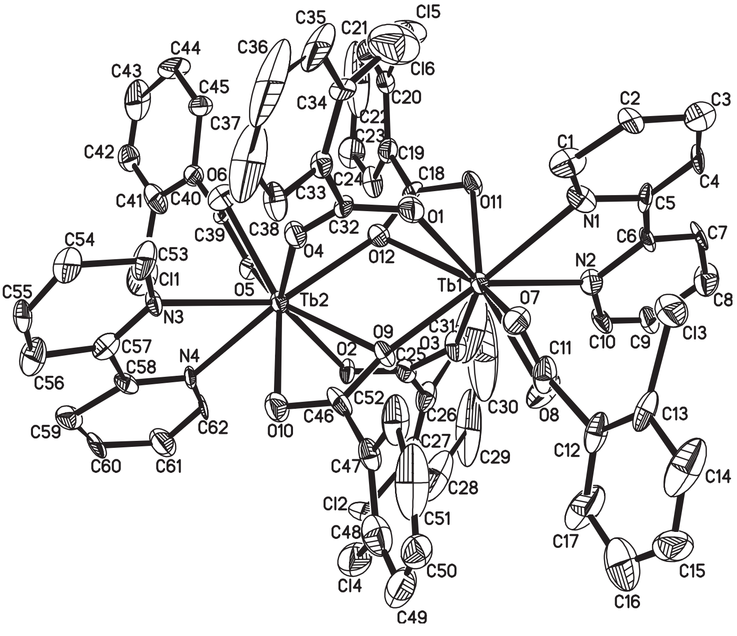

Figure 4. Molecular structure of **2**. All hydrogen atoms have been omitted for clarity; the thermal ellipsoids are shown at the 30% probability level.

from one 2,2′-bipy. The TbO_7N_2 may be described as a distorted monocapped square-antiprism. O1, O3, O9, O11 and O7, O8, N1, N2 form the upper and lower planes with mean deviations of 0.1155 and 0.0809 Å from the two planes, respectively. The dihedral angle between the upper and lower planes is 1.6° and atom O12 caps the upper plane. The Tb1–O bond distances range from 2.328(10)–2.586(10) Å with an average of 2.424 Å. The Tb1–N bond distances are 2.612(11) and 2.536(12) Å, respectively, with an average of 2.574 Å. The distance between $Tb1^{3+}$ ions is 3.9910(3) Å. The bond angles of O–Tb1–O range from 51.0(3)–146.2(4)° and that of N1–Tb1–N2 is 62.0(4)°.

The two complexes differ from $[Tb(2\text{-}FBA)_3 \cdot 2,2'\text{-bipy}]_2$ (2-FBA = 2-fluorobenzoate) [13], which contains three independent binuclear molecules in the asymmetric unit and $[Tb(2\text{-}MBA)_3phen]_2$ (2-MBA = 2-methylbenzoate) [14], which contains two independent binuclear molecules in the asymmetric unit with the same coordination environments of Tb^{3+}. However, the reported terbium benzoate (BA) complexes, $[Tb(BA)_3(2,2'\text{-bipy})]_2$ [11] and $[Tb(BA)_3(phen)]_2$ [12], contain one binuclear molecule in the asymmetric unit with coordination numbers of eight and nine, respectively.

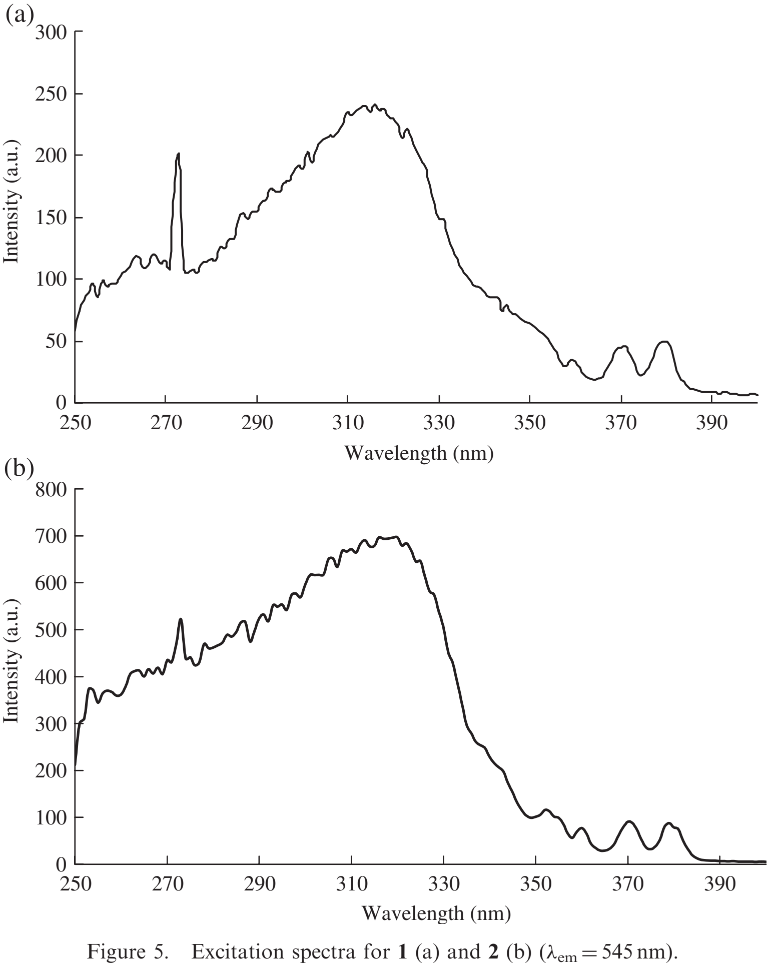

Figure 5. Excitation spectra for **1** (a) and **2** (b) ($\lambda_{em} = 545$ nm).

The structures of $[Tb(BA)_3(2,2'\text{-bipy})]_2$ and $[Tb(BA)_3(phen)]_2$ are similar to those of (a) and (b) in **1**, respectively. Lanthanide complexes with benzoic acid and its derivatives have different structures from different coordination modes of carboxylates. Most lanthanide mono-aromatic acid complexes with 2,2′-bipy or phen contain one type of binuclear molecule in the asymmetric unit; complexes like **1** with two independent molecules in the asymmetric unit are less reported.

3.2. *Luminescence properties*

Both complexes emit intense green fluorescence under ultraviolet light. The solid-state excitation and luminescence spectra of the two complexes were recorded at room temperature. Excitation was measured in the range 250–400 nm (figure 5). Fluorescence was observed in a range 400–700 nm by selected excitation wavelength at 325 nm for both complexes (figure 6). The luminescence properties of the two complexes are similar to other terbium complexes with characteristic $^5D_4 \rightarrow {}^7F_j$ ($j = 6$–3) transitions of Tb^{3+}; the positions of their emission bands are similar. In the luminescence spectra, there are four main emission peaks centered at 489, 544, 583, and 620 nm for **1** and 489,

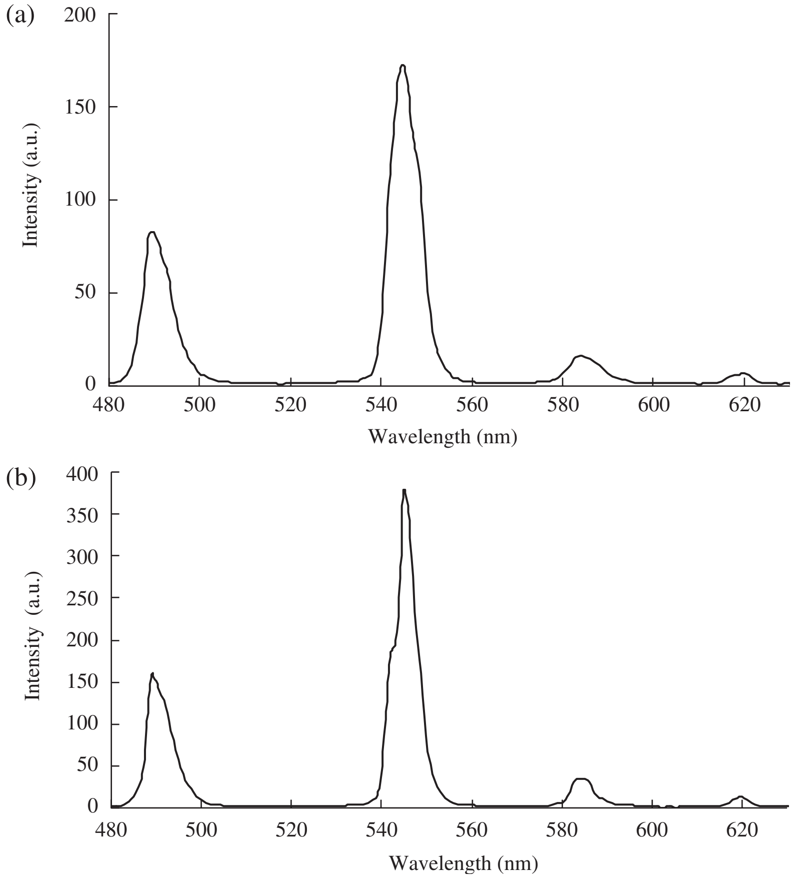

Figure 6. Fluorescence spectra for **1** (a) and **2** (b) ($\lambda_{ex} = 325$ nm).

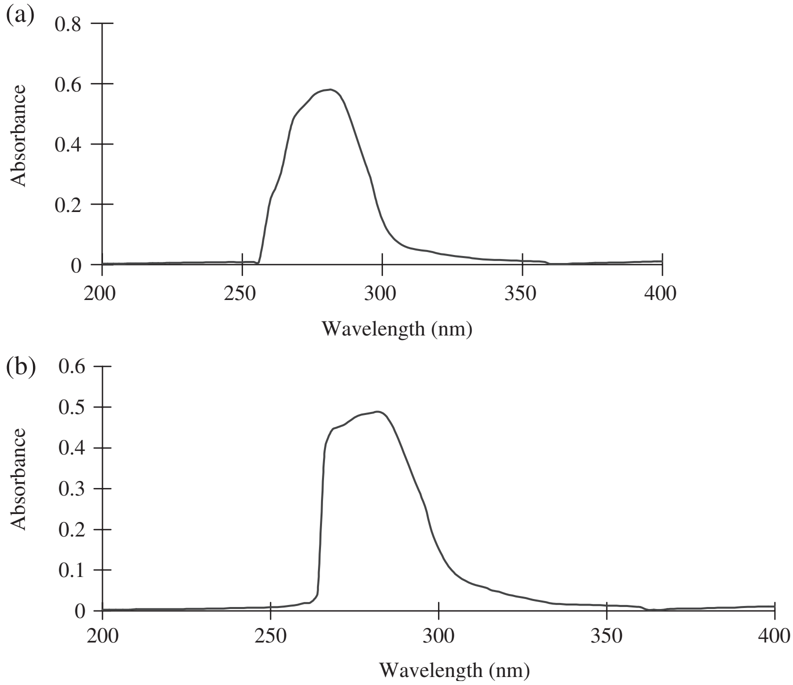

Figure 7. UV absorption spectra for **1** (a) and **2** (b) ($c = 1.00 \times 10^{-5}\,\mathrm{mol\,L^{-1}}$).

545, 584, and 620 nm for **2**, originating from $^5D_4 \rightarrow {}^7F_6$, $^5D_4 \rightarrow {}^7F_5$, $^5D_4 \rightarrow {}^7F_4$, and $^5D_4 \rightarrow {}^7F_3$ transitions of Tb^{3+}, respectively. The luminescence band arising from $^5D_4 \rightarrow {}^7F_5$ transition is most intense. The ligands absorb ultraviolet light and transfer energy to the Tb^{3+} ion in complex; the absorption band at 289 nm for **1** and 288 nm for **2** in UV absorption spectra in DMF solution ($1.0 \times 10^{-5}\,\mathrm{mol\,L^{-1}}$) correspond to the $\pi \rightarrow \pi^*$ transition of the ligands (figure 7).

3.3. *Thermogravimetric analysis*

Thermal behaviour of the complexes was studied in the temperature range from 25–1000°C, as shown in figure 8. The DTA curves indicate that decomposition begins at 264°C for **1** and 256°C for **2** and ends at 482°C for **1** and 523°C for **2**. The TG curves show two steps of weight loss. The first weight loss of 16.82% for **1** and 19.45% for **2** corresponds to release of one ethanol molecule and two 2,2′-bipy molecules (calculated: 16.60%) for **1** and two 2,2′-bipy molecules (calculated: 19.98%) for **2**. Then carboxylate ligands decompose. The total weight loss is 82.65% for **1** and 75.87% for **2**, indicating the complexes decompose to Tb_4O_7 (calculated: 82.68% for **1** and 76.09% for **2**). In general, ternary lanthanide benzoate complexes containing aromatic diimine ligand (such as 2,2′-bipy or phen) show high thermal stability and decompose above 200°C. The aromatic diimine ligand is lost first. For example, phen is lost first in thermal decompositions of $[Tb_2(BA)_6(phen)_2]$ [12] and $[Tb_2(2\text{-}MBA)_6(phen)_2]$ [14]. In such complexes, the Tb–N (aromatic diimine) distance is longer than that of Tb–O (carboxylate), so Tb–N bonds are less stable and are easily lost.

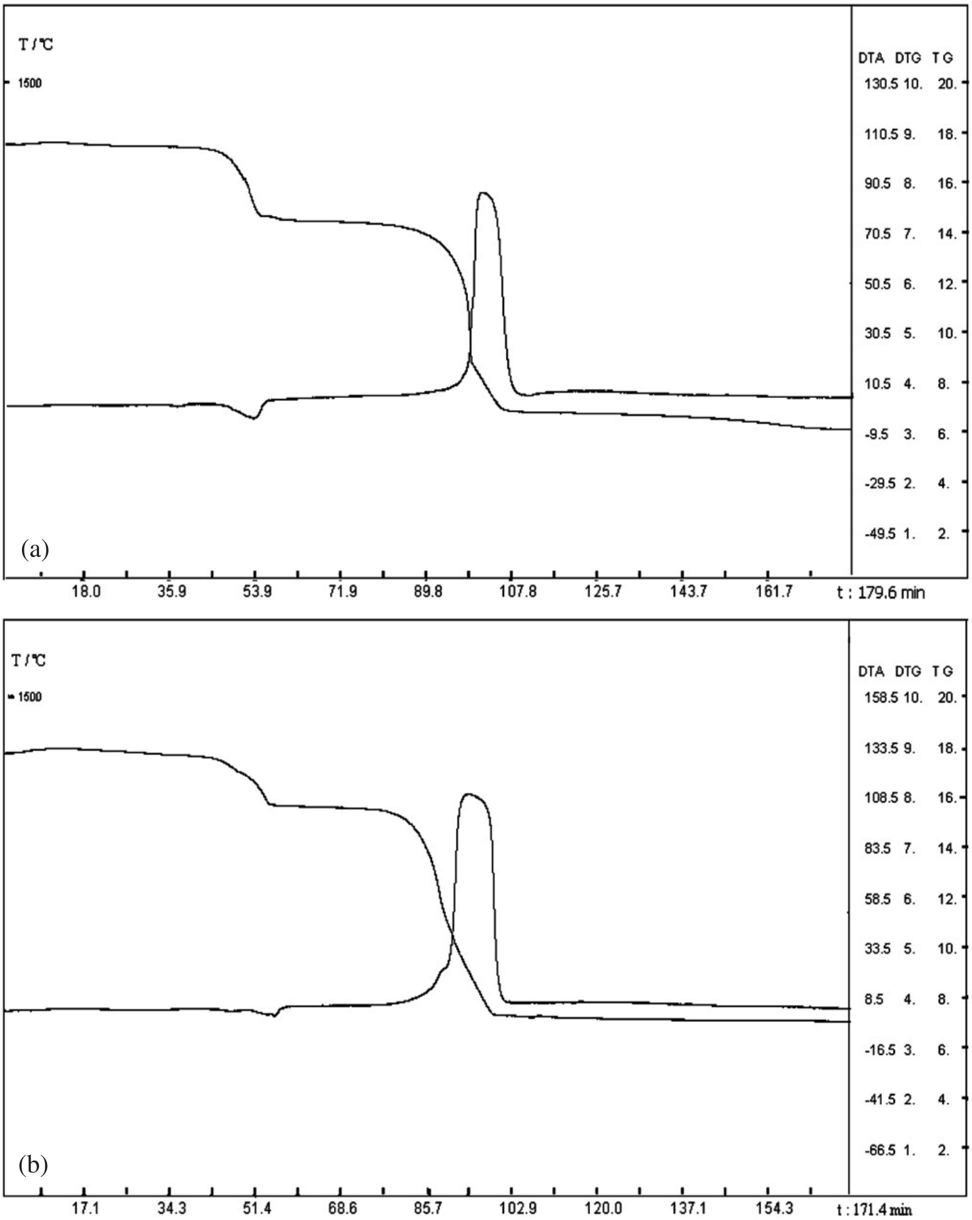

Figure 8. TG-DTA curves for **1** (a) and **2** (b).

Supplementary data

CCDC-633484 for **1** and 633483 for **2** contain the supplementary crystallographic data for this article. These data can be obtained free of charge from CCDC, 12 Union Road, Cambridge, CB2 1EZ, UK; Fax: +44(0) 1223-336033; Email: deposit@ccdc.cam.ac.uk.

Acknowledgements

We are grateful to the Natural Science Foundation of Beijing (No. 2073022), the Science and Technology Program, Beijing Municipal Education Commission (KM200510028007), the Young Mainstay Teachers Foundation of Beijing Municipal Universities and the Beijing Key Lab of Nano-photonics and Nano-structure.

References

[1] J.L. Weissman. *Chem. Phys.*, **10**, 214 (1942).
[2] T.M. Reineke, M. Eddaoudi, M. Fehr, D. Kelley, O.M. Yaghi. *J. Am. Chem. Soc.*, **121**, 1651 (1999).
[3] B. Barja, R. Baggio, M.T. Garland, P.F. Aramendia, O. Peña, M. Perec. *Inorg. Chim. Acta*, **346**, 187 (2003).
[4] B. Barja, P. Aramendia, R. Baggio, M.T. Garland, O. Peña, M. Perec. *Inorg. Chim. Acta*, **355**, 183 (2003).
[5] P.C.R. Soares-Santos, H.I.S. Nogueira, J. Rocha, V. Félix, M.G.B. Drew, R.A.S. Ferreira, L.D. Carlos, T. Trindade. *Polyhedron*, **22**, 3529 (2003).
[6] M.C. Yin, C.C. Ai, L.J. Yuan, C.W. Wang, J.T. Sun. *J. Mol. Struct.*, **691**, 33 (2004).
[7] R.F. Wang, S.P. Wang, S.K. Shi, J.J. Zhang. *J. Coord. Chem.*, **55**, 215 (2002).
[8] C. Seward, N.X. Hu, S.N. Wang. *J. Chem. Soc., Dalton Trans.*, 134 (2001).
[9] L. Oyang, H.L. Sun, X.Y. Wang, J.R. Li, D.B. Nie, W.F. Fu, S. Gao, K.B. Yu. *J. Mol. Struct.*, **740**, 175 (2005).
[10] C.H. Ye, H.L. Sun, X.Y. Wang, J.R. Li, D.B. Nie, W.F. Fu, S. Gao. *J. Solid State Chem.*, **177**, 3735 (2004).
[11] L.J. Xu, S.P. Wang, Z.H. Gao, R.F. Wang. *Acta Cryst., Section E*, **62**, m1853 (2006).
[12] R.F. Wang, S.P. Wang, S.K. Shi, J.J. Zhang. *Chinese J. Struct. Chem.*, **23**, 1300 (2004).
[13] X. Li, Z.Y. Zhang, Y.Q. Zou. *Eur. J. Inorg. Chem.*, **14**, 2903 (2005).
[14] R.F. Wang, S.P. Wang, S.K. Shi, J.J. Zhang. *Rare Metals*, **23**, 103 (2004).
[15] G.M. Sheldrick. Phase Annealing in SHELX-97: direct methods for larger structures, *Acta Cryst.*, **A46**, 467 (1990).
[16] G.M. Sheldrick. *SHELXL97, Program for X-ray Crystal Structure Solution*, University of Göttingen, Germany (1997).